FYS4411/FYS9411 – Computational Physics II

Time-Dependent Hartree-Fock Theory on a 1D Harmonic Laser Trap with 2 Electrons

Jonas Boym Flaten & Simon Elias Schrader
University of Oslo

June 1, 2021

Abstract

We derive and implement Hartree-Fock (HF) solvers for two electrons in a one-dimensional harmonic oscillator of strength $\omega = 0.25$ a.u. using the harmonic oscillator energy eigenstates as atomic orbital basis. Using Restricted Hartree-Fock (RHF), we have found an expectation energy $E_{\text{RHF}} = 1.1796$ a.u., and using General Hartree-Fock (GHF) $E_{\text{GHF}} = 0.84504$ a.u. There are qualitative differences in the shape of the ground state spatial densities and the molecular orbitals, with the RHF solution having a single maximum and the GHF solution having two maxima. We also derive and implement time-dependent Hartree-Fock (TDHF) solvers with respect to an external time-dependent laser field. We have used this to reproduce the results by Zanghellini et al.[1] with our RHF solution showing similarities to their HF solution, and our GHF solution qualitatively resembling their full configuration interaction (FCI) solution. Finally, we found a single peak in the Fourier spectrum of the dipole moment at $\omega_d = 0.25 \pm 0.01$ a.u. after turning off the laser, which is in accordance with the Harmonic Potential Theorem[2]. We briefly discuss the need of a large enough atomic orbital basis set for TDHF calculations.

1 Introduction

Recently, the ever-increasing power of commercially available computers and the development of high performance computation libraries such as NumPy[3] and SciPy[4] has made simulations of the time evolution of quantum systems feasible on personal computers. These simulations can be used to obtain more insight into a system than ground-state simulations are capable of, as they predict the dynamics of a system, which can then also be used to infer time-independent variables such as excitation energies, as well as the population of states after a time-dependent Hamiltonian has acted on a system.

There are two main aims in this report: Firstly, we derive and implement a general Hartree-Fock (GHF) and a spin-restricted Hartree-Fock (RHF) solver to simulate two electrons trapped in a one-dimensional harmonic oscillator potential and compare the two approaches. Secondly, we derive and implement a time-dependent Hartree-Fock (TDHF) solver with an external, time dependent sinusoidal potential that represents a laser in the dipole-approximation, with the full model Hamiltonian given in (2.1). The data obtained from these simulations was used to infer information about the system's energy spectrum, which we are not able to calculate through normal Hartree-Fock means. In both cases we compare our results to those obtained by Zanghellini et al.[1], which serves as our benchmark.

In section 2.1, we declare our model and the parameters that enter into the simulations. We then go on to derive and discuss theoretical aspects: In sections 2.2 and 2.3, we introduce the single-

determinant Slater approximation and the resulting Hartree-Fock algorithm used to minimize the expected energy of the trial determinant, followed by the description of the TDHF algorithm in section 2.4. In section 2.5, we discuss inclusion of spin and describe the additional restrictions made to the trial determinant in the RHF algorithm. Thereafter we present how to calculate expected values of observables of interest and how Fourier transforms of time-dependent expected values can give information about the excited energy spectrum of the system in section 2.6, before finally going through the computational implementation of the algorithm in section 2.7.

In section 3, we present our results and discuss relevant aspects of their implications, including comparisons with [1]. We summarise and conclude our findings in section 4.

2 Theory & Methods

2.1 Model

The system we consider in this article consists of two electrons in a one-dimensional harmonic oscillator subject to a laser field, for simplicity referred to as a (harmonic) laser trap. The Hamiltonian in position basis is

$$H = \sum_{i}^{N} \left(-\frac{\hbar^2}{2m}\frac{\partial^2}{\partial x_i^2} + \frac{1}{2}m\omega^2 x_i^2 + \sum_{j>i}^{N} \frac{1}{4\pi\epsilon}\frac{e^2}{x_{ij}+a} - e x_i \mathscr{E}[t]\sin[\lambda\omega t] \right) \tag{2.1}$$

where x_i is the position of electron i, $x_{ij} = |x_i - x_j|$ is the distance between electrons i and j, t is time and N is the number of electrons. Furthermore $\hbar$ is the reduced Planck constant, m is the electron mass, ω is the strength of the harmonic trap potential, ϵ is the permittivity (of free space) and a is a screening length of the Coulomb interaction to prevent a singularity when the electrons come too close. Finally $\mathscr{E}[t]$ is the amplitude and λ is the relative frequency of the electric laser field, and $\mathscr{E}[t]$ is defined so that the laser turns off at a specified time T,

$$\mathscr{E}[t] = \begin{cases} \mathscr{E} & \text{for} \quad t < T \\ 0 & \text{for} \quad t \geq T. \end{cases} \tag{2.2}$$

The clutter of physical constants in (2.1) can be removed by introducing suitable units for the involved quantities. This also makes the quantities dimensionless, which is desirable in computational physics. Introducing to this end $\frac{4\pi\epsilon\hbar^2}{me^2}$ as unit of length, $m(\frac{e^2}{4\pi\epsilon\hbar})^2$ as unit of energy, $\frac{\hbar^3}{m}(\frac{4\pi\epsilon}{e^2})^2$ as unit of time (and hence $\frac{m}{\hbar^3}(\frac{e^2}{4\pi\epsilon})^2$ as unit of trap strength and frequency) and finally $(\frac{me^2}{\hbar^2})^2(\frac{1}{4\pi\epsilon})^3$ as unit of electrical field. These units are known as *atomic units* or *Hartree*, or a.u. in shorthand notation, and we will refer to them as such. The Hamiltonian then takes the dimensionless form

$$H = -\frac{1}{2}\left(\frac{\partial^2}{\partial x_1^2} + \frac{\partial^2}{\partial x_2^2}\right) + \frac{1}{2}\omega\left(x_1^2 + x_2^2\right) + \frac{1}{x_{12}+a} - (x_1 + x_2)\mathscr{E}[t]\sin[\lambda\omega t] \tag{2.3}$$

where the sums in (2.1) were written out for $N = 2$. This dimensionless form, along with its dimensionless parameters ω, a, $\mathscr{E}$, λ and T as well as dimensionless length, energy and time in general, is used throughout this article and the associated code, but the units introduced above should be kept in mind when presenting the results. In [1], the parametric values considered are $\omega = 0.25$, $a = 0.25$, $\mathscr{E} = 1.0$, $\lambda = 8.0$ and $T = \infty$, and so these values will naturally be used when comparing results, but we will also consider a finite $T = \frac{\lambda\omega}{2\pi}$ to see how the "aftermath" of the laser can provide further insight into the system.

2.2 Slater determinants

The simplest possible Hamiltonian to model a system of N interacting particles is

$$H = \sum_{i}^{N} h_i + \sum_{i}^{N} \sum_{j>i}^{N} u_{ij}, \tag{2.4}$$

where h_i is a one-body Hamilton operator h working only on the particle with index i in the many-body Hilbert product space and u_{ij} is a two-body interaction operator u working on the particles with index i and j. Such Hamiltonians serve as the starting point for many-body quantum mechanical calculations and are often used to model many-body quantum systems. Indeed the model Hamiltonian introduced in (2.3) has this very form.

Considering a Hamiltonian of the form (2.4), we want to find an approximate fermionic N-body wave eigenfunction. In spin-position basis this eigenfunction takes the form $\Phi[\mathbf{q}] = \Phi[\mathbf{q}_1, \mathbf{q}_2, \ldots, \mathbf{q}_N]$ with $\mathbf{q}_i = [\mathbf{r}_i, s_i]$, where $\mathbf{r}_i$ is the position of the ith particle and s_i its spin component along some given spin axis. If there were no interaction term in the Hamiltonian, so that it had the even simpler form

$$H = \sum_{i}^{N} h_i, \tag{2.5}$$

an intuitive approach would be to split it into one-body terms and find solutions $\{\phi_i\}$ to the corresponding one-body Schrödinger equation, such that $h\phi_i = \varepsilon_i \phi_i$. A candidate for the total wave eigenfunction would then be the so-called *Hartree product*

$$\Phi[\mathbf{q}_1, \mathbf{q}_2, \mathbf{q}_3, \ldots \mathbf{q}_N] = \phi_1[\mathbf{q}_1]\phi_2[\mathbf{q}_2] \ldots \phi_N[\mathbf{q}_N], \tag{2.6}$$

and the corresponding energy would be simply $E = \sum_{i=1}^{N} \varepsilon_i$. However, by the Pauli exclusion principle any fermionic many-body wave function needs to be antisymmetric under the exchange of two particles, that is

$$\Phi[\mathbf{q}_1, \ldots, \mathbf{q}_i, \ldots, \mathbf{q}_j, \ldots, \mathbf{q}_N] = -\Phi[\mathbf{q}_1, \ldots, \mathbf{q}_j, \ldots, \mathbf{q}_i, \ldots, \mathbf{q}_N] \qquad \forall \quad i \neq j \in \{1, \ldots, N\}, \tag{2.7}$$

which is clearly not the case for the Hartree product above. The simplest remedy for this is to make an antisymmetric sum of permutations of the Hartree product. Because any determinant of a matrix switches sign under the exchange of two rows or columns, such an antisymmetric sum can be written concisely as a so-called *Slater determinant*,

$$\Phi[\mathbf{q}_1, \mathbf{q}_2, \ldots, \mathbf{q}_N] = \frac{1}{\sqrt{N!}} \begin{vmatrix} \phi_1[\mathbf{q}_1] & \phi_2[\mathbf{q}_1] & \cdots & \phi_N[\mathbf{q}_1] \\ \phi_1[\mathbf{q}_2] & \phi_2[\mathbf{q}_2] & \cdots & \phi_N[\mathbf{q}_2] \\ \vdots & \vdots & \ddots & \vdots \\ \phi_1[\mathbf{q}_N] & \phi_2[\mathbf{q}_N] & \cdots & \phi_N[\mathbf{q}_N] \end{vmatrix}. \tag{2.8}$$

The factor $\frac{1}{\sqrt{N!}}$ makes the Slater determinant normalised as long as the set of one-body wave eigenfunctions $\{\phi_i\}$ is orthonormal, which it can always be made to be. Because the Slater determinant is nothing but an antisymmetric sum of Hartree products constructed from the same one-body wave eigenfunctions, it follows that the Slater determinant is also a total wave eigenfunction with the corresponding energy $E = \sum_i^N \varepsilon_i$.

As discussed above, Slater determinants are exact energy eigenfunctions of many-body Hamiltonians of the form (2.5) with inherent fermionic antisymmetry. However, many-body Hamiltonians of the form (2.4) have interaction terms, and in this case Slater determinants will generally *not* be able to represent the proper energy eigenfunction of the system. (After all, Slater determinants span only the single product part of the full many-body Hilbert product space in which the states of the system

live.) But they *can* serve as a starting point and often turn out to be a good approximation. This is the underlying idea for *Hartree-Fock theory*, which is presented further in section 2.3.

Before discussing Hartree-Fock-theory we introduce some notation related to Slater determinants. Let $|\Phi\rangle$ be a Slater determinant and h_i the one-body operator h acting only on the ith particle. Then it can be shown that, for an operator sum of the form $\mathcal{O}_1 = \sum_{i=1}^{N} h_i$,

$$\langle\Phi|\mathcal{O}_1|\Phi\rangle = \sum_{i}^{N} \langle i|h|i\rangle \tag{2.9}$$

where we denote

$$\langle i|\, h\, |j\rangle \equiv \langle\phi_i|\, h\, |\phi_j\rangle = \int \phi_i^*[\mathbf{q}_1] h[\mathbf{q}_1] \phi_j[\mathbf{q}_1] d\mathbf{q}_1. \tag{2.10}$$

Similarly, for a two-body operator sum of the form $\mathcal{O}_2 = \sum_{i=1}^{N}\sum_{j>i}^{N} u_{ij}$ it can be shown that

$$\langle\Phi|\mathcal{O}_2|\Phi\rangle = \frac{1}{2}\sum_{i}^{N}\sum_{j}^{N} \langle ij||ij\rangle \tag{2.11}$$

where we denote

$$\langle ij|kl\rangle \equiv \langle\phi_i\phi_j|\, u\, |\phi_k\phi_l\rangle = \int\int \phi_i^*[\mathbf{q}_1]\phi_j^*[\mathbf{q}_2] u[\mathbf{q}_1,\mathbf{q}_2]\phi_k[\mathbf{q}_1]\phi_l[\mathbf{q}_2] d\mathbf{q}_1 d\mathbf{q}_2 \tag{2.12}$$

and

$$\langle ij||kl\rangle \equiv \langle ij|kl\rangle - \langle ij|lk\rangle\,. \tag{2.13}$$

With the introduced notation and a Hamiltonian of the general form (2.4), the expected energy of the Slater determinant $|\Phi\rangle$ is given by

$$E = \langle\Phi|H|\Phi\rangle = \sum_{i}^{N} \langle i|h|i\rangle + \frac{1}{2}\sum_{i}^{N}\sum_{j}^{N} \langle ij||ij\rangle. \tag{2.14}$$

2.3 Time-independent Hartree-Fock theory

The Variational Principle of quantum mechanics states that the ground state energy E_0 of a system is bounded by

$$E_0 \leq \langle\Psi|H|\Psi\rangle\,, \tag{2.15}$$

where $|\Psi\rangle$ is *any* normalised quantum state in the Hilbert state space of the system. This incredibly versatile fact provides a general way of estimating the ground state of a quantum system: Define some trial state $|\Psi\rangle$ which depends on a certain amount of parameters, and minimise the energy bound $\langle\Psi|H|\Psi\rangle$ with respect to these parameters. This minimal energy bound is the closest you get to the true ground state energy for that family of trial states.

Hartree-Fock theory invokes the Variational Principle on a quantum many-body system of N interacting fermions with a Hamiltonian of the form (2.4) by choosing a (normalised) Slater determinant $|\Phi\rangle$ as the trial state. As noted in the previous section, Slater determinants span only part of the full many-body Hilbert product space, but the resulting approximate ground state energy, hereafter denoted as the *Hartree-Fock energy* E_{HF}, is often good when the fermion interaction is weak compared to other mechanisms in the system.

In section 2.2, Slater determinants were introduced as the exact fermionic energy eigenstates of a many-body Hamiltonian of the form (2.5), with no interaction terms. In this case, the Slater determinant had to be constructed from energy eigenstates of the corresponding one-body Schrödinger equation. However, the only variation allowed in such a Slater determinant is the choice of which

of the one-body energy eigenstates to include in the determinant, which would simply be the N one-body energy eigenstates with the lowest energy. The resulting Hartree-Fock energy would of course be a fair estimate of the ground state energy, but a much better estimate can be found by allowing the Slater determinant to be constructed by *any* set of N one-body states $|\phi_i\rangle$. As long as these one-body states are orthonormal, the Slater determinant takes the form (2.8) in spin-position basis, even though the one-body states are no longer necessarily energy eigenstates of the one-body Hamiltonian h.

Hartree-Fock theory concerns variation of the very one-body states $|\phi_i\rangle$ themselves to minimise the energy bound $\langle\Phi|H|\Phi\rangle$. To make this variation explicit, we introduce another set of M basis states $|\chi_a\rangle$ for the one-body state space. *This* set could very well be the energy eigenstates of h, and in many cases it will be (including this article), but in general it could be any basis set – even one which is not orthonormal. The one-body states to be varied can then be expanded as

$$|\phi_i\rangle = \sum_a^M C_{ai}\,|\chi_a\rangle\,, \tag{2.16}$$

and it now becomes clear what to vary – namely the expansion coefficients C_{ai}. As is the custom within Hartree-Fock theory, we will refer to the set of one-body states $|\phi_i\rangle$ from which the trial Slater determinant is built as the *molecular orbitals* and the basis set $|\chi_a\rangle$ as the *atomic orbitals* of the system. We also introduce a customary notation in which the letters i,j,k... are used for summation indices running from 1 to N, through the molecular orbitals included in the Slater determinant, while the letters a,b,c,... are used for summation indices running from 1 to M, through the full number of atomic orbitals in the basis. This notation makes the size of the involved sums and matrices a bit more transparent.

Equation (2.14) provides the energy bound of the trial Slater determinant as a function of the molecular orbitals. Expanding these into atomic orbitals using (2.16) we get an expression for the energy bound as a function of the expansion coefficients:

$$\begin{aligned}\langle\Phi|H|\Phi\rangle &= \sum_i^N \langle\phi_i|h|\phi_i\rangle + \frac{1}{2}\sum_{i,j}^N \langle\phi_i\phi_j||\phi_i\phi_j\rangle \\ &= \sum_{a,b}^M\sum_i^N C_{ai}^* C_{bi}\,\langle\chi_a|\,h\,|\chi_b\rangle + \frac{1}{2}\sum_{a,b,c,d}^M\sum_{i,j}^N C_{ai}^* C_{bj}^* C_{ci} C_{dj}\langle\chi_a\chi_b||\chi_c\chi_d\rangle.\end{aligned} \tag{2.17}$$

(Here $\langle\chi_a\chi_b||\chi_c\chi_d\rangle$ follows the notation introduced in section 2.2 so that

$$\langle\chi_a\chi_b||\chi_c\chi_d\rangle = \langle\chi_a\chi_b|\,u\,|\chi_c\chi_d\rangle - \langle\chi_a\chi_b|\,u\,|\chi_d\chi_c\rangle = u_{abcd} \tag{2.18}$$

for the specific two-body interaction operator u in consideration. u is $\frac{1}{r_{ij}+a}$ in our model Hamiltonian (2.3).)

The bound (2.17) is almost ready to be minimised, however the molecular orbitals are not to be varied totally freely. Indeed, the formula (2.14) only holds true when the molecular orbitals are *orthonormal*, so they should be varied with the constraint that they be kept orthonormal. Such a constrained variation is achieved by introducing a Lagrangian function

$$\begin{aligned}L =\ & \langle\Phi|H|\Phi\rangle - \sum_{i,j}^N \alpha_{ij}^*\Big(\langle\phi_i|\phi_j\rangle - \delta_{ij}\Big) \\ =\ & \sum_{a,b}^M\sum_i^N C_{ai}^* C_{bi}\,\langle\chi_a|\,h\,|\chi_b\rangle + \frac{1}{2}\sum_{a,b,c,d}^M\sum_{i,j}^N C_{ai}^* C_{bj}^* C_{ci} C_{dj}\langle\chi_a\chi_b||\chi_c\chi_d\rangle - \sum_{i,j}^N \alpha_{ij}^*\Big(\sum_a^M C_{ai}^* C_{aj} - \delta_{ij}\Big)\end{aligned} \tag{2.19}$$

in which the Lagrange multipliers α_{ij}^* enforce the orthonormal constraint. The Lagrangian L should be minimised with respect to both the expansion coefficients *and* the Lagrange multipliers. In appendix A.1 this minimisation is carried out, leading to the matrix *Roothaan-Hall equation*

$$\boxed{F}\boxed{C} = \boxed{C}\boxed{\varepsilon}, \tag{2.20}$$

where the elements of the so-called *Fock matrix* $\boxed{F}$ are

$$F_{ab} = \langle\chi_a|\, h\, |\chi_b\rangle + \sum_{c,d}^{M} P_{cd}\langle\chi_a\chi_d||\chi_b\chi_c\rangle \tag{2.21}$$

in terms of the *density matrix* $\boxed{P}$ defined as

$$\boxed{P} = \boxed{C}\boxed{C}^\dagger. \tag{2.22}$$

The density matrix will turn out to contain the actual *physics* of the optimised Slater determinant in the sense that all expected values for the system observables depend on the coefficients only through $\boxed{P}$, in a similar way to the Fock matrix. We will demonstrate this further in section 2.6, but note already that the expected energy, which is what we have referred to as the energy bound (2.17), can be recast as

$$E = \langle\Phi|H|\Phi\rangle = \sum_{a,b}^{M} P_{ab}\,\langle\chi_b|\, h\, |\chi_a\rangle + \frac{1}{2}\sum_{a,b,c,d}^{M} P_{ab}P_{cd}\langle\chi_b\chi_d||\chi_a\chi_c\rangle. \tag{2.23}$$

When an optimised Slater determinant has been found, its expected energy takes the lowest possible value for any Slater determinant constructed from M atomic orbitals. This energy is what we refer to as the Hartree-Fock energy E_{HF}, and we can use the formula (2.23).

The Roothaan-Hall equation (2.20) is nothing but an eigenequation stating that the columns of the coefficient matrix $\boxed{C}$ should be eigenvectors of the Fock matrix $\boxed{F}$ with eigenvalues given along the diagonal of $\boxed{\varepsilon}$. However the elements of the Fock matrix are not constant – they dependend on the coefficient matrix $\boxed{C}$ – so it is not a linear eigenequation that can be solved by normal means. Instead the custom is to deal with it iteratively, by repeatedly solving eigenequations of approximate Fock matrices. This iterative procedure, known from the olden days as *self-consistent field (SCF) iteration* or simply Hartree-Fock iteration, goes as follows:

1. Make an initial guess for the coefficient matrix $\boxed{C}$ (such as a cropped identity matrix corresponding to the N lowest-energy atomic orbitals as initial molecular orbitals).
2. Calculate the density matrix $\boxed{P}$ and then the Fock matrix $\boxed{F}$ using the definitions (2.22) and (2.21).
3. Solve the eigenequation $\boxed{F}\boxed{C^+} = \boxed{C^+}\boxed{\varepsilon^+}$ to obtain the $M \times M$ eigenmatrix $\boxed{C^+}$ of $\boxed{F}$, and pick the N lowest-eigenvalue columns of this matrix as the new coefficient matrix $\boxed{C}$.
4. Repeat 2 and 3 until some convergence criterion is met.
5. Calculate the Hartree-Fock energy E_{HF} given by the formula (2.23), or any other expected value of interest.

Through this procedure, the orthonormal constraint $\boxed{C}^\dagger\boxed{C} = \boxed{I}$, which is emphatically also required for the minimisation, can be automatically fulfilled: As the Fock matrix $\boxed{F}$ is Hermitian by definition, its eigenvectors, some of which will make up the new coefficient matrix $\boxed{C}$ at every iteration, can *always* be made orthonormal, and most eigensolvers do this by default.

There are many possible convergence criteria for when to stop Hartree-Fock iteration. The simplest criterion is to stop after a set maximum number of iterations, which by no means guarantees convergence at all. Better criteria would be to ensure that the change in the coefficient matrix $\boxed{C}$, the

density matrix $\boxed{P}$ or the expected energy E between two successive iterations is smaller than some given threshold. The "safest" convergence criterion however would be to check the Roothaan-Hall equation (2.20) itself by calculating the difference between its right and left side at each iteration. Convergence could be said to be achieved when this difference is smaller than a given threshold. An equivalent convergence criterion can be found by considering the conjugate transpose of the Roothaan-Hall equation,

$$\boxed{C}^\dagger \boxed{F} = \boxed{\varepsilon}\boxed{C}^\dagger, \tag{2.24}$$

which along with the Roothaan-Hall equation (2.20) itself should be fulfilled at the minimum. But then we can do the subtraction (2.20)$\boxed{C}^\dagger$ − $\boxed{C}$(2.24) to obtain

$$\boxed{F}\boxed{P} - \boxed{P}\boxed{F} = \boxed{0}. \tag{2.25}$$

In words then, the Fock matrix and the density matrix will commute at the minimum. Hence we can simply check this commutator, which is a computationally faster criterion as the eigenvalue matrix $\boxed{\varepsilon}$ will not ever need to be stored. Note that this convergence check (as well as a direct Roothaan-Hall check) should be made between point 2 and 3 above to ensure that the Fock matrix $\boxed{F}$ is from another iteration than $\boxed{C}$ and $\boxed{P}$. If the Fock matrix is from the same iteration, the convergence criterion is fulfilled trivially and would lead to instant fake convergence.

One final note before we move on is that Hartree-Fock iteration is actually not guaranteed to converge at all. The Hartree-Fock method relies on minimisation of a multi-dimensional function through iteration, and should be expected to be subject to the same issues as other iterative schemes such as the Newton method. Depending on the choice of initial coefficients $\boxed{C}$, the iteration could very well end up caught in a local minimum or some saddle point. Because the coefficients are tightly linked to the basis, the atomic orbitals $|\chi_a\rangle$, the choice of atomic orbitals will also affect convergence. Especially if the initial choice of molecular orbitals are simply the N lowest-energy atomic orbitals as suggested above, it makes intuitive sense that the Hartree-Fock iteration will converge faster if the atomic orbitals are already similar to the optimal molecular orbitals. Thus, as with all iterative schemes a clever initial guess should be made.

The Hartree-Fock theory presented so far concerns finding an approximation to the ground state energy of a quantum many-body system by the Variational Principle (2.15) on a trial Slater determinant. As long as the system Hamiltonian has the form (2.4), the iterative method described in the previous section *will* (at proper convergence) find the lowest possible energy for a Slater determinant state constructed for a given number of atomic orbitals M. In the process it even finds the lowest-energy Slater determinant state itself, through its molecular orbital coefficients. Hence Hartree-Fock theory in a broader sense is not just about finding an approximate *ground state energy*, but rather finding an approximate *ground state*, from which one can calculate approximate expected values for all other observables of interest. Since most quantum systems spend much time in their ground state, these expected values are useful as they tell a lot about the system itself.

2.4 Time-dependent Hartree-Fock theory

Our model Hamiltonian (2.3) has the right form, and so we can use Hartree-Fock theory to find the approximate Slater determinant ground state. Our model is time-dependent however, and so we are also interested in the time-development of the system. There is nothing preventing us from using Hartree-Fock iteration to find the instantaneous approximate ground state at any time t – however this will not give us much insight into the time development of the system, as it will only tell us how the approximate ground state shifts with time. When a time-dependent quantum system evolves however, it will typically oscillate between the ground state and excited states, governed by the (time-dependent) Schrödinger equation. We cannot in general expect a Slater determinant to solve the Schrödinger equation, but we can once again find a Slater determinant as the approximate

solution by constructing a Lagrangian and minimising it. In this case the Lagrangian takes the form

$$\begin{aligned} L &= \langle\Phi|H - \iota\frac{\partial}{\partial t}|\Phi\rangle - \sum_{i,j}^{N}\alpha_{ij}^{*}\Big(\langle\phi_i|\phi_j\rangle - \delta_{ij}\Big) \\ &= \sum_{a,b}^{M}\sum_{i}^{N} C_{ai}^{*}C_{bi}\langle\chi_a|\,h\,|\chi_b\rangle + \frac{1}{2}\sum_{a,b,c,d}^{M}\sum_{i,j}^{N} C_{ai}^{*}C_{bj}^{*}C_{ci}C_{dj}\langle\chi_a\chi_b||\chi_c\chi_d\rangle - \iota\sum_{a}^{M}\sum_{i}^{N} C_{ai}^{*}\dot{C}_{ai} \\ &\quad - \sum_{i,j}^{N}\alpha_{ij}^{*}\Big(\sum_{a}^{M} C_{ai}^{*}C_{aj} - \delta_{ij}\Big), \end{aligned} \tag{2.26}$$

where ι is the imaginary unit and we use a dot to denote the time derivative. C_{ai} are the molecular orbital coefficients as defined in (2.16) and α_{ij}^{*} are Lagrange multipliers enforcing the constraint that the molecular orbitals be orthonormal, but note now that both the coefficients and the Lagrange multipliers are now functions of time, and that we minimise the expected value $\langle\Phi|H - \iota\frac{\partial}{\partial t}|\Phi\rangle$ to ensure that our Slater determinant evolves with the Schrödinger equation as well as possible. Another difference which follows from this is that we do not just want to minimise the Lagrangian L at one specific point in time – we want to minimise it with respect to a whole *span* of time. It makes sense then to minimise the integral of the Lagrangian with respect to time, the so-called *action*

$$S = \int L\delta t. \tag{2.27}$$

When this integral is minimised with respect to both the coefficients and the Lagrange multipliers, the Lagrangian keeps as small as possible throughout the whole time span in the sense that its time-average (which equals the action up to a scaling factor) is minimal. In appendix A.2 the full minimisation is carried out and shown to result in the time-dependent Roothaan-Hall equation

$$\iota\dot{\boxed{C}} = \boxed{F}\boxed{C}, \tag{2.28}$$

which governs the time evolution of the coefficient matrix $\boxed{C}$ and hence the molecular orbitals of the system. We can then expand the Hartree-Fock procedure presented in section 2.3 to include a typical time propagation of the system. As the time-dependent Hartree-Fock equation (2.30) gives a coupled non-linear system of differential equations, it can only be solved approximately with a numerical integration scheme. After finding an initial Hartree-Fock ground state through points 1 to 4 of the previous section, one would proceed with the following steps to propagate it in time:

1. Declare the time-dependent Fock matrix $\boxed{F}$ as a matrix function of both the coefficient matrix $\boxed{C}$ and time t.
2. Declare $-\iota\boxed{F}\boxed{C}$ as a matrix function of both the coefficient matrix $\boxed{C}$ and time t.
3. Feed this matrix function into a numerical matrix integrator of preference along with a time interval Δt (and possibly a time step δt).
4. Obtain the time-propagated coefficient matrix $\boxed{C}$, use it to calculate the time-propagated density matrix $\boxed{P}$ and then the time evolution of any observable of interest.

Because the molecular orbitals are constrained to be orthonormal at every point in time, one can use similar expressions for the expected values of the system as in the time-independent case, given in section 2.6.

To conclude our treatment of time-dependent Hartree-Fock theory, we let ourselves intrigue by the appealing form of the convergence criterion (2.25) derived in the previous section. This is nothing

but the Roothaan-Hall equation expressed through $\boxed{P}$, and we can make a similar equation from the time-dependent Roothaan-Hall equation (2.28) by noting that its conjugate transpose is

$$-\imath\dot{\boxed{C}}^\dagger = \boxed{C}^\dagger \boxed{F}, \tag{2.29}$$

so that the subtraction (2.28)$\boxed{C}^\dagger - \boxed{C}$(2.29) results in

$$\imath\dot{\boxed{P}} = \boxed{F}\boxed{P} - \boxed{P}\boxed{F}. \tag{2.30}$$

The density matrix turns out to evolve based on its commutator with the Fock matrix. This might distress the keen reader, for we learned from equation (2.25) that in the Hartree-Fock ground state $\boxed{F}$ and $\boxed{P}$ actually commute. It would seem then that an initial Hartree-Fock ground state stays grounded forever. However note that this is not the case as the Fock matrix $\boxed{F}$ normally depends on time not only through the density matrix, but also through some external potential in the one-body Hamiltonian h. Sure, the density matrix will not change at the exact initial point in time if our initial state has been found through Hartree-Fock iteration. In the next instant however, the Hamiltonian has changed so that the initial ground state is no longer the instantaneous Hartree-Fock ground state of the Hamiltonian. Then the commutator between $\boxed{F}$ and $\boxed{P}$ is no longer zero, and time evolution begins.[1]

2.5 Spin-restricted Hartree-Fock theory

In our treatment of Hartree-Fock theory so far, nothing has been specified about the basis set of atomic orbitals $|\chi_a\rangle$, other than the fact that there are M of them. These orbitals are indeed arbitrary. Of course the choice will directly change the matrix elements of h and u with respect to the atomic orbitals, but then the optimal coefficients $\boxed{C}$ will change accordingly, so that we in principle end up with the same Hartree-Fock energy after Hartree-Fock iteration. The choice of atomic orbitals will hence only affect the speed of convergence as discussed at the end of section 2.3.

The choice of atomic orbitals can however simplify the amount of matrix elements and coefficients involved, especially with regard to spin. We call the M atomic orbitals $|\chi_a\rangle$ *spin-restricted* if they can be separated as

$$|\chi_a^s\rangle = |\psi_a\rangle\,|s\rangle\,, \tag{2.31}$$

where $|\psi_a\rangle$ is some spatial basis of $\frac{M}{2}$ one-body states and $|s\rangle$ is the electronic spin basis – either $|\uparrow\rangle$ or $|\downarrow\rangle$. (A tensor product is implied by juxtaposition of states, that is $|\psi_a\rangle\,|s\rangle \equiv |\psi_a\rangle \otimes |s\rangle$.) In this case each atomic orbital has a definite spin direction along the given spin axis, hence the name, and there are two orbitals corresponding to each spatial state $|\psi_a\rangle$. Spin-restricted orbitals are interesting because typical molecular Hamiltonians do not include the spin operator, as the effects of electron–electron spin interaction are negligible. In fact most model Hamiltonians are formulated in spatial basis, omitting spin entirely. Thus one usually starts with some *spatial* one-body basis $|\psi_a\rangle$ from which one will have to construct an atomic orbital basis by including the spin part of the proper state space. When including spin one could of course mix spin up and down as one pleases in the orbitals, but the simplest way of including it is to construct spin-restricted orbitals like (2.31). We will do just this in this article, and we will furthermore use the energy eigenstates of the one-body Hamiltonian h as our spatial part $|\psi_a\rangle$, as hinted briefly in section 2.3.

There is a deeper reason that spin-restricted orbitals are interesting. When the model Hamiltonian H is independent of spin, the spin operator commutes with H, and then the energy eigenstates of

[1] The keen but distressed reader would perhaps also be calmed by the following insight: Were the Fock matrix *not* to depend on time through anything other than the density matrix – well, then the Hamiltonian of the system would not be time-dependent at all, and so an initial ground state should indeed stay grounded forever.

the system should really be simultaneous eigenstates of both energy and spin.[2] In other words, spin-restricted atomic orbitals are a natural choice of basis for the energy eigenstates of the system.

From here on we assume that our M atomic orbitals are spin-restricted and defined through (2.31). The most general way of constructing N molecular orbitals $|\phi_i\rangle$ from these is simply to combine

$$|\phi_i\rangle = \sum_a^{\frac{M}{2}} \sum_s C_{ai}^s \, |\chi_a^s\rangle = \sum_a^{\frac{M}{2}} \sum_s C_{ai}^s \, |\psi_a\rangle \, |s\rangle \qquad \text{for all} \quad i \in \{1, \ldots, N\}, \tag{2.32}$$

where it is implicit that the spin index s runs through $\downarrow$ and $\uparrow$. When we defined the molecular orbital expansion in (2.16), we used this general definition – up until now we just simplified it to a single sum over M coefficients C_{ai} running from C_{1i} to C_{Mi}, and assuming some ordering of the spin-restricted atomic orbitals into one single array. When using this general definition of the molecular orbitals, hereafter referred to as *general Hartree-Fock theory* (or simply GHF), we alternate between spin up and down so that

$$|\chi_{2a-1}\rangle \equiv \left|\chi_a^{\downarrow}\right\rangle = |\psi_a\rangle \, |\downarrow\rangle \quad \text{and} \quad |\chi_{2a}\rangle \equiv \left|\chi_a^{\uparrow}\right\rangle = |\psi_a\rangle \, |\uparrow\rangle \qquad \text{for all} \quad a \in \{1, \ldots, M\}, \tag{2.33}$$

that is, atomic orbitals of odd index have spin down while atomic orbitals of even index have spin up, and two successive orbitals have the same spatial component.

Note however that with the GHF definition the molecular orbitals lose the definite spin of the atomic orbitals, as each molecular orbital is a superposition of atomic orbitals with spin up and spin down. In *spin-restricted Hartree-Fock theory* (or simply RHF) the N molecular orbitals are instead constructed to keep the definite spin direction,

$$|\phi_i^s\rangle = \sum_a^{\frac{M}{2}} C_{ai} \, |\chi_a^s\rangle = \sum_a^{\frac{M}{2}} C_{ai} \, |\psi_a\rangle \, |s\rangle \qquad \text{for all} \qquad i \in \left\{1, \ldots, \frac{N}{2}\right\}, \tag{2.34}$$

where one should note that there are two molecular orbitals, one with spin $\downarrow$ and one with spin $\uparrow$, corresponding to each index i. It is clear then that the RHF approach by construction yields Slater determinants which *are* eigenstates of the spin operator S^2, as derived in [5]. This is not necessarily the case for GHF Slater determinants, which are made up of spin-mixed molecular orbitals. Even though a GHF solution could in principle end up with just the right combination of spin-mixed molecular orbitals to be an eigenstate of spin, this is not guaranteed. We say that GHF solutions are prone to *spin contamination*, while RHF solutions keep *spin purity*.

From a glimpse it would seem that RHF solutions are the only reasonable choice – after all, as discussed, any true energy eigenstate of a spin-independent Hamiltonian should be spin pure, so RHF is the only choice making physical sense. However remember that we are *anyway* not handling the actual energy eigenstates here – we are only working with Slater determinant approximations, which do *not* fathom the whole state space of the system. The unrestricted GHF solutions span out a larger part of the whole state space – they have a larger coefficient matrix $\boxed{C}$, which means more flexibility – and will in general result in a lower Hartree-Fock energy. This means that if one is interested in approximating the ground state energy *only*, GHF would be the best choice.

It remains to show how RHF's spin-restricted molecular orbitals as defined in (2.34) affect the Roothaan-Hall equations (2.20) and (2.28) as well as the expressions (2.22) and (2.21) for the density and Fock matrices. RHF turns out to simplify the computational procedure greatly, as we only need a coefficient matrix $\boxed{C}$ of size $\frac{M}{2} \times \frac{N}{2}$, which then results in density and Fock matrices $\boxed{P}$ and $\boxed{F}$ of size $\frac{M}{2} \times \frac{M}{2}$. Smaller matrices mean a smaller Roothaan-Hall system of equations to solve,

[2] Even in the case of degenerate energy eigenstates, simultaneous spin eigenstates can always be constructed by a suitable transformation without affecting the physics – a freedom similar to the unitary transformation of the molecular coefficients $\boxed{C}$ discussed in appendices A.1 and A.2.

both for the eigensolver in Hartree-Fock iteration 2.3 as well as for the numerical integrator in the Hartree-Fock time evolution 2.4. In appendix A.3 it is derived that in addition to this change in dimensions, the atomic orbital matrix elements will also change following the formulas

$$\sum_s \langle \chi_a^s | \, h \, | \chi_b^s \rangle = 2 \langle \psi_a | \, h \, | \psi_b \rangle \,, \tag{2.35}$$

and

$$\sum_{s,p} \langle \chi_a^s \chi_b^p || \chi_c^s \chi_d^p \rangle = 4 \langle \psi_a \psi_b | \, u \, | \psi_c \psi_d \rangle - 2 \langle \psi_a \psi_b | \, u \, | \psi_d \psi_c \rangle \tag{2.36}$$

when the spin parts are summed out. This leads to a slight change in the Fock matrix, which now has elements

$$F_{ab} = \langle \psi_a | \, h \, | \psi_b \rangle + \sum_{c,d}^{\frac{M}{2}} P_{cd} \Big(2 \langle \psi_a \psi_d | \, u \, | \psi_b \psi_c \rangle - \langle \psi_a \psi_d | \, u \, | \psi_c \psi_b \rangle \Big). \tag{2.37}$$

Furthermore, the expected energy given in (2.23) becomes

$$E = \langle \Phi | H | \Phi \rangle = \sum_{a,b}^{\frac{M}{2}} 2 P_{ab} \langle \psi_b | \, h \, | \psi_a \rangle + \sum_{a,b,c,d}^{\frac{M}{2}} P_{ab} P_{cd} \Big(2 \langle \psi_b \psi_d | \, u \, | \psi_a \psi_c \rangle - \langle \psi_b \psi_d | \, u \, | \psi_c \psi_a \rangle \Big). \tag{2.38}$$

and the other expected value expressions provided in the next section should also change following (2.35) and (2.36) in a similar fashion. All other matrix definitions and equations however, such as (2.22), (2.20) and (2.28), take the exact same form in RHF as in GHF as long as one keeps the halving of dimensions in mind.

2.6 Observables

Having discussed the full Hartree-Fock machinery in sections 2.3–2.5, we conclude our derivations of Hartree-Fock theory by listing appropriate expressions for the expected value of some observables of interest that we will calculate and discuss in section 3. Keep in mind that we provide the expressions in their GHF form, but the RHF form can easily be deduced by halving the dimensions M and N while transforming atomic orbital matrix elements using (2.35) and (2.36) as explained in section 2.5.

- The **spatial particle density** is, for a general N-particle function, defined as

$$\rho[\mathbf{r}] = \sum_i^N \sum_{s_i \in \{\downarrow\uparrow\}} \int \cdots \int |\phi[\mathbf{q}, \mathbf{q}_2, ... \mathbf{q}_N]|^2 d\mathbf{r}_2 \cdots d\mathbf{r}_N, \tag{2.39}$$

  which means that we sum out the spins of all particles and integrate out the positions of all particles but one. For a Slater determinant this expression becomes particularly easy,

$$\rho[\mathbf{r}] = \frac{1}{N} \Big(|\phi_1[\mathbf{r}]|^2 + |\phi_2[\mathbf{r}]|^2 + \cdots + |\phi_N[\mathbf{r}]|^2 \Big) = \frac{1}{N} \sum_{i=1}^N |\phi_i[\mathbf{r}]|^2. \tag{2.40}$$

  The proof goes as follows:

  When writing out the Slater determinant explicitly, it is a sum containing $N!$ terms. The probability distribution $|\phi[\mathbf{q}_1, \mathbf{q}_2, ... \mathbf{q}_N]|^2$ will thus contain $(N!)^2$ terms. However, $(N!)^2 - N!$ of these terms will have at least one set of particle indices interchanged, such as

$$(\phi_1[\mathbf{q}_j] \dots \phi_k[\mathbf{q}_l] \dots)^* \, (\phi_1[\mathbf{q}_j] \dots \phi_k[\mathbf{q}_m] \dots) \,.$$

  Due to the orthogonality of the molecular orbitals, these $(N!)^2 - N!$ terms will not contribute. For the $N!$ contributions that are left, for each molecular orbital ϕ_i there will be $(N-1)!$

contributions where $\mathbf{q}_1$ *is placed in molecular orbital* ϕ_i*, as there are generally* $(N-1)!$ *ways to arrange the other particle indices* $\mathbf{q}_j$ *into the other molecular orbitals. Integrating out all indices but* $\mathbf{q}_1$ *in addition to* s_1 *and using the normalization of the Slater determinant* $\frac{1}{\sqrt{N!}}$*, we are left with a prefactor of* $\frac{(N-1)!}{N!} = \frac{1}{N}$ *for each of the* N *molecular orbitals, which gives us eq.* (2.40).

The total particle density can then be obtained by multiplying eq. (2.40) by the number of particles (which is 2 in our case). When recasting this in terms of atomic orbitals, calculating $|\phi_i[\mathbf{r}]|^2$ is in principle straightforward. The only thing one has to be careful about is how spin is summed out, which should be done the following way:

$$|\phi_i[\mathbf{r}]|^2 = \sum_{s\in\{\uparrow\downarrow\}} |\phi_i[\mathbf{q}]|^2 = \sum_{s,s_i\in\{\downarrow\uparrow\}} \sum_{a}^{\frac{M}{2}} |C_{ai}^{s_i}\psi_a[\mathbf{r}]\,\langle s|s_i\rangle|^2 = \sum_{a}^{\frac{M}{2}} \left(\left|C_{ai}^{\uparrow}\psi_a[\mathbf{r}]\right|^2 + \left|C_{ai}^{\downarrow}\psi_i[\mathbf{r}]\right|^2 \right). \tag{2.41}$$

- The expected **dipole moment d** of the system is defined as

$$\mathbf{d} = -\sum_{i=1}^{N} \langle\Phi|\mathbf{r}_i|\Phi\rangle\,. \tag{2.42}$$

Because $\sum_i \mathbf{r}_i$ is a one-body operator of the form $\mathcal{O}_\mathbf{1} = \sum_{i=1}^N h_i$, we use (2.9) to get

$$\mathbf{d} = -\sum_{i=1}^{N} \langle\phi_i|\mathbf{r}_i|\phi_i\rangle = -\sum_{a,b}^{M}\sum_{i=1}^{N} C_{ai}^* C_{bi}\,\langle\chi_a|\,\mathbf{r}\,|\chi_b\rangle = -\sum_{a,b}^{M} P_{ab}\,\langle\chi_b|\,\mathbf{r}\,|\chi_a\rangle \tag{2.43}$$

Observe that the contributions of most of the sum are necessarily equal to zero. This is because $\langle\chi_b|\,\mathbf{r}\,|\chi_a\rangle$ is necessarily zero when $|\chi_a\rangle$ has spin up and $|\chi_b\rangle$ has spin down or vice versa, so only the elements with identical spin contribute.

- The expected **energy** E of the system is given by equation (2.23), which can also be rewritten to depend on the Fock matrix $\boxed{F}$ given in (2.21):

$$\begin{aligned}
E &= \sum_{a,b}^{M} P_{ab}\,\langle\chi_b|\,h\,|\chi_a\rangle + \frac{1}{2}\sum_{a,b,c,d}^{M} P_{ab}P_{cd}\langle\chi_b\chi_d||\chi_a\chi_c\rangle \\
&= \sum_{a,b}^{M} P_{ab}\left(\langle\chi_b|\,h\,|\chi_a\rangle + \frac{1}{2}\sum_{c,d}^{M} P_{cd}\langle\chi_b\chi_d||\chi_a\chi_c\rangle\right) \\
&= \sum_{a,b}^{M} P_{ab}\left(\frac{1}{2}\langle\chi_b|\,h\,|\chi_a\rangle + \frac{1}{2}\left(\langle\chi_b|\,h\,|\chi_a\rangle + \sum_{c,d}^{M} P_{cd}\langle\chi_b\chi_d||\chi_a\chi_c\rangle\right)\right) \\
&= \frac{1}{2}\sum_{ab}^{M} P_{ab}\,(h_{ba} + F_{ba})\,.
\end{aligned} \tag{2.44}$$

Here we introduced the one-body Hamiltonian matrix $\boxed{h}$ with elements

$$h_{ab} = \langle\chi_a|\,h\,|\chi_b\rangle\,. \tag{2.45}$$

- The **overlap** between two states $|\Psi'\rangle$ and $|\Psi\rangle$ is defined as $\langle\Psi'|\Psi\rangle$. Let $|\Phi'\rangle$ and $|\Phi\rangle$ be two Slater determinants with possibly different molecular orbitals. The overlap between two non-orthonormal Slater determinants, as derived in the article by Plasser et al.[6], is given by

$$\langle\Phi'|\Phi\rangle = \begin{vmatrix} \langle\phi_1'|\phi_1\rangle & \dots & \langle\phi_1'|\phi_N\rangle \\ \vdots & \ddots & \vdots \\ \langle\phi_N'|\phi_1\rangle & \dots & \langle\phi_N'|\phi_N\rangle \end{vmatrix} \equiv \det\boxed{\Gamma}. \tag{2.46}$$

If, as in our case, the same atomic basis is used for both Slater determinants and the atomic basis is orthonormal, the matrix elements simplify to

$$\left\langle \phi'_j | \phi_i \right\rangle = \sum_{a,b}^{M} C'^{*}_{bi} C_{aj} \left\langle \chi_b | \chi_a \right\rangle = \sum_{a}^{M} C'^{*}_{ai} C_{aj} \tag{2.47}$$

We recognise thus that $\boxed{\Gamma} = \boxed{C'}^{\dagger}\boxed{C}$, where $\boxed{C'}$ and $\boxed{C}$ are the $M \times N$ coefficient matrices of the Slater determinants. For the absolute overlap squared, the so-called **fidelity** Γ, this means that

$$\Gamma = |\langle \Phi' | \Phi \rangle|^2 = \left| \det \boxed{\Gamma} \right|^2 = \left| \det \left[\boxed{C'}^{\dagger} \boxed{C} \right] \right|^2 . \tag{2.48}$$

The *initial state fidelity* $|\langle \Phi_0 | \Phi[t] \rangle|^2$ measures the overlap between the evolving state $|\Phi[t]\rangle$ and the initial state $|\Phi_0\rangle \equiv |\Phi[0]\rangle$ of a system. In the case of time-dependent Hartree-Fock theory, the initial state is often (such as in this report) just the Hartree-Fock ground state of the system, so we can also refer to this as the *ground state fidelity*. In the results section 3 we will refer to it simply as the "overlap", but from the context this slight abuse of terms should be clear.

We proceed to develop some final expressions for time-dependent observables of our system. In general, the expressions for these have the same form as above, just with time-dependent matrices $\boxed{C}$,$\boxed{P}$ and $\boxed{F}$. (The matrices for h and u are in atomic orbital basis and hence time-independent.) However some discussion of time-dependent overlaps is in order.

As defined in our model (2.1) and its laser amplitude (2.2), the laser is on until the point in time T and then turned off. When it is on, the laser will move the system out of its ground state, and so many expectation values will become time dependent. In general, when the time-dependent part of a Hamiltonian is turned off, the system follows the general equation of time evolution $|\Psi[T+t]\rangle$, found by separating out time-dependent coefficients in the time-dependent Schrödinger equation:

$$|\Psi[T+t]\rangle = e^{-iHt} |\Psi[T]\rangle = \sum_{n=0}^{\infty} c_n[T] e^{-iE_n t} |\psi_n\rangle . \tag{2.49}$$

Here $|\psi_n\rangle$ are the eigenfunctions of the time-independent Hamilton operator.

Now, let $\hat{O}$ be any operator. The time-dependent expected value of operator $\hat{O}$ is

$$\begin{aligned} O[t] = \langle \Psi[T+t] | \hat{O} | \Psi[T+t] \rangle &= \sum_{n=0}^{\infty} \sum_{m=0}^{\infty} c^*_n[T] c_m[T] e^{i(E_m - E_n)t} \langle \psi_n | \hat{O} | \psi_m \rangle \\ &\equiv \sum_{n=0}^{\infty} \sum_{m=0}^{\infty} c^*_n[T] c_m[T] e^{-i\Delta E_{nm} t} O_{nm}, \end{aligned} \tag{2.50}$$

where we defined $\Delta E_{nm} = E_n - E_m$. Similarly, the time-dependent overlap between the state at the time the laser was turned off and at a time later, reads

$$\begin{aligned} \langle \Psi[T+t] | \Psi[T] \rangle &= \sum_{n=0}^{\infty} \sum_{m=0}^{\infty} c^*_n[t] c_m[T] \langle \psi_n | \psi_m \rangle \\ &= \sum_{n=0}^{\infty} \sum_{m=0}^{\infty} c^*_n[T] c_m[T] e^{-iE_n t} \delta_{nm} = \sum_{n=0}^{\infty} |c_n[T]|^2 e^{-iE_n t}, \end{aligned} \tag{2.51}$$

$$\begin{aligned} |\langle \Psi(t+T) | \Psi[T] \rangle|^2 &= \left(\sum_{n=0}^{\infty} |c_n[T]|^2 e^{-iE_n t} \right) \left(\sum_{m=0}^{\infty} |c_m[T]|^2 e^{-iE_m t} \right)^* \\ &= \sum_{n=0}^{\infty} \sum_{m=0}^{\infty} |c_n[T]|^2 |c_m[T]|^2 e^{-i\Delta E_{nm} t} \end{aligned} \tag{2.52}$$

Observe that this will necessarily be a real number, as we can regroup

$$|c_n[T]|^2 |c_m[T]|^2 \left(e^{-i\Delta E_{nm}t} + e^{-i\Delta E_{mn}t}\right) = 2|c_m[T]|^2 |c_n[T]|^2 \cos\left[\Delta E_{nm}t\right] \tag{2.53}$$

We see in both cases that the right hand side looks like a (discrete) Fourier transform. Thus, Fourier transforming the time-dependend expectation values and the overlap should give the system's transition energies ΔE, even when the states are not explicitly known, in form of the peaks in the Fourier spectrum.

In this article, the observable of interest is mainly the dipole moment, and time evolution is done through the Roothaan-Hall equation (2.28). For a plain harmonic oscillator, one only observes transitions up or down one state, as $\langle n|\hat{x}|m\rangle = C(\delta_{n,m+1} + \delta_{n,m-1})$ for some constant C. According to the *Harmonic Potential Theorem*[2], N interacting electrons in a harmonic oscillator potential with frequency ω will only absorb radiation at the harmonic oscillator frequency ω independently on the number of electrons and the interaction, which implies that there should only be one peaks in the Fourier spectrum of the time-dependent expectation value of an operator at multiples of ω, that is, $\Delta E_{ij} = n\omega$ for $n \in \mathbb{N}_0$.

2.7 Numerical implementation

We implemented Hartree-Fock solvers in both Python and Julia, using the formulas and equations from time-independent and time-dependent, general as well as spin-restricted, Hartree-Fock theory as derived in the sections above. All the code developed for this project is available on GitHub[3], and both codes are well commented for easy examination. The Python code was developed earlier on and includes functionality for Fourier analysis of the results, and so it was used to obtain all the plots of section 3. However both the Python and the Julia codes ended up giving the same results, validating the correctness of our two implementations and the suitability of the numerical schemes chosen.

As mentioned in section 2.5 we use $\frac{M}{2}$ energy eigenstates of h as the spatial parts $|\psi_a\rangle$ of the atomic orbitals. The derived Hartree-Fock formulas and equations all rely on having the matrix elements of the operators h, u and x with respect to the atomic orbital basis. Hence a discretisation and numerical solution of the one-body system $h|\psi\rangle = \varepsilon|\psi\rangle$ is in order. We consider an atomic orbital basis of size $M = 20$ and a finite discretised spatial grid of size 1001 spanning from $x = -10$ to $x = 10$. These numbers for M and x match the ones used in [1]. In order to increase accuracy, we will however increase both the number of atomic basis orbitals and the grid length, but this will be stated explicitly. The spatial basis functions and the relevant matrix elements of h, u and x were all calculated with the `quantum_systems` package by Øyvind S. Schøyen[4] which was integrated in our Python and Julia implementations.

We did not implement any test functions, as we deemed getting the same values with our Python and Julia codes as and results that match with Zanghellini et al.[1] as well as theoretical and physical implications a sufficient way to check that our implementations are correct. While our code was developed with the model Hamiltonian (2.3) in mind, only minor adaptions would need to be made to adjust it to any system with a Hamiltonian of the general form (2.4).

2.7.1 Python implementation

In Python we implemented a solver class which has functions for solving the Roothaan-Hall equation (2.20) for $N = 2$ electrons in a harmonic oscillator potential and evolve it in time. There are two classes, `GHFSolverSystem` and `RHFSolverSystem`, where the latter is a subclass of the former. As the `RHFSolverSystem` solves the restricted Roothan-Hall equation described in section 2.5, the coefficient

[3] Our codes can be found in the `code` folder at https://github.com/schraderSimon/ComputationalPhysics2-Project2

[4] The `quantum_systems` package can be accessed on https://github.com/Schoyen/quantum-systems

matrix is of size $\frac{M}{2} \times \frac{M}{2}$. As most functions assume a matrix size of $M \times M$, the coefficient matrix needs to be read out and passed to a new `GHFSolverSystem`-object if more than the ground state energy is of interest.

Computational efficiency. To make calculations reasonably fast, we rely heavily on the use of NumPy[3], such as n-dimensional arrays and the `einsum`-function. We also use NumPy's implementation of the Fourier transform.

Time evolution. To perform the time evolution, we use SciPy's[4] `complex_ode` integrator with the `zvode` algorithm. This numerical integrator does not work for matrices, hence it is essential to reshape the coefficient matrix $\boxed{C}$ back and forth between an array for integration, but a matrix for matrix multiplication. Even though this is more expensive, we time evolve the full eigenmatrix $\boxed{C^+}$ instead of the relevant submatrix $\boxed{C}$, however computation time is still manageable and we deemed it unnecessary to improve further.

2.7.2 Julia implementation

Since Julia is not an object-oriented language, our main Julia script `HarmonicLaserTrapHartreeFock_C.jl` consists of two functions, `find_HF_state` which takes in an algorithm string (either `"GHF"` or `"RHF"`) as well as the necessary parametric values and calculates the Hartree-Fock energy, and `find_HF_evolution` which takes in additional values for the time span and the resolution of time plots. Parametric values for the harmonic laser trap are organised in `HarmonicLaserTrap1D` structs, which are passed to the main functions along with algorithm and output arguments.

Computationally, the Julia code relies on similar algorithms to the ones used in the Python script. The matrix diagonalisation and numerical integration involved were done using the functions `eigvecs` and `solve` from the native Julia packages `LinearAlgebra` and `DifferentialEquations`, respectively.

The Julia code is built to work easily with the Julia REPL, in which structs for relevant laser traps can be declared and passed to multiple function calls with different parametric input. The keyword arguments `text_output` and `plot_output` specify what output to be returned by the script. Some plots and output from the Julia code can be found in the folder `code/Julia/output/` on GitHub.

3 Results & Discussion

3.1 Hartree-Fock ground state energy

For the energy calculations, the parametric values given in sections 2.1 and 2.7 where used. We used the atomic basis orbitals as an initial guess for the overlap matrix – that is, the initial guess for the coefficient matrix is the identity matrix $\boxed{C^+} = \boxed{I}$ as suggested in the algorithm of section 2.3.

Figure 1 shows the energy of our system found with both GHF and RHF for the first 100 SCF (Hartree-Fock) iterations.

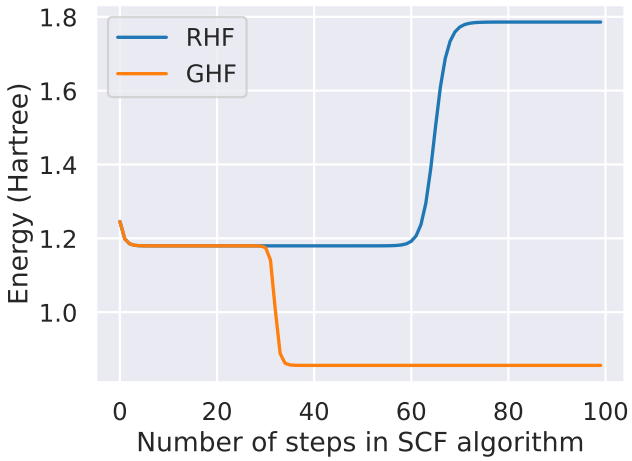

Figure 1: *Ground state expectation energy E of the Slater determinant as function of the number of steps in the SCF procedure for spin-restricted Hartree-Fock (RHF) and general Hartree-Fock (GHF) for the first 100 iterations. The GHF algorithm finds a lower-lying minimum than the RHF minimum. Not shown in the graph is that there is an even lower lying minimum for the GHF algorithm, found after $N \approx 1200$ iterations.*

We see that the energy of both RHF and GHF stabilizes at $E_{\text{RHF}} = 1.1796$, which is the same HF-energy as found in the article by Zanghellini et al.[1] In the rest of the article, we will call this state the *RHF solution*. This is also the minimum energy of the RHF energy, which goes to a higher energy after ~ 60 steps.[5] The GHF algorithm, however, finds a lower energy state after ~ 30 steps, with $E = 0.85580$. After ~ 1200 steps, an even lower lying energy state is found, with $E_{\text{GHF}} = 0.84504$. This state will be called the *GHF solution* in the rest of this article. This result for the energy is rather impressive – compared to the ground state energy of the FCI solution found by Zanghellini et. al, $E_{\text{FCI}} = 0.8247$, the relative deviation is only $\frac{E_{\text{GHF}} - E_{\text{FCI}}}{E_{\text{FCI}}} \approx 2.5\%$.

3.2 Hartree-Fock ground state spatial density

Figure 2 shows the RHF and the GHF ground state (total) spatial electron densities $2\rho[x]$. This, and all future calculations of the RHF solution, were made with the solution of the RHF algorithm after 25 steps, while 5000 steps were used for the GHF solution. The GHF solution after 25 steps is virtually identical to the RHF solution after 25 steps in terms of energy, electron density and the initial time-dependent behaviour, but we discovered some instabilities, and thus we opted to use the solution from the RHF algorithm.

[5] We cannot fully explain why this happens, but we suppose that it is due to numerical instabilities in the SCF procedure. As the whole aim of the HF equations is to minimise the energy, full convergence of SCF iteration is not as good as getting the lowest possible energy, especially when spin symmetry is already accounted for, as with RHF.

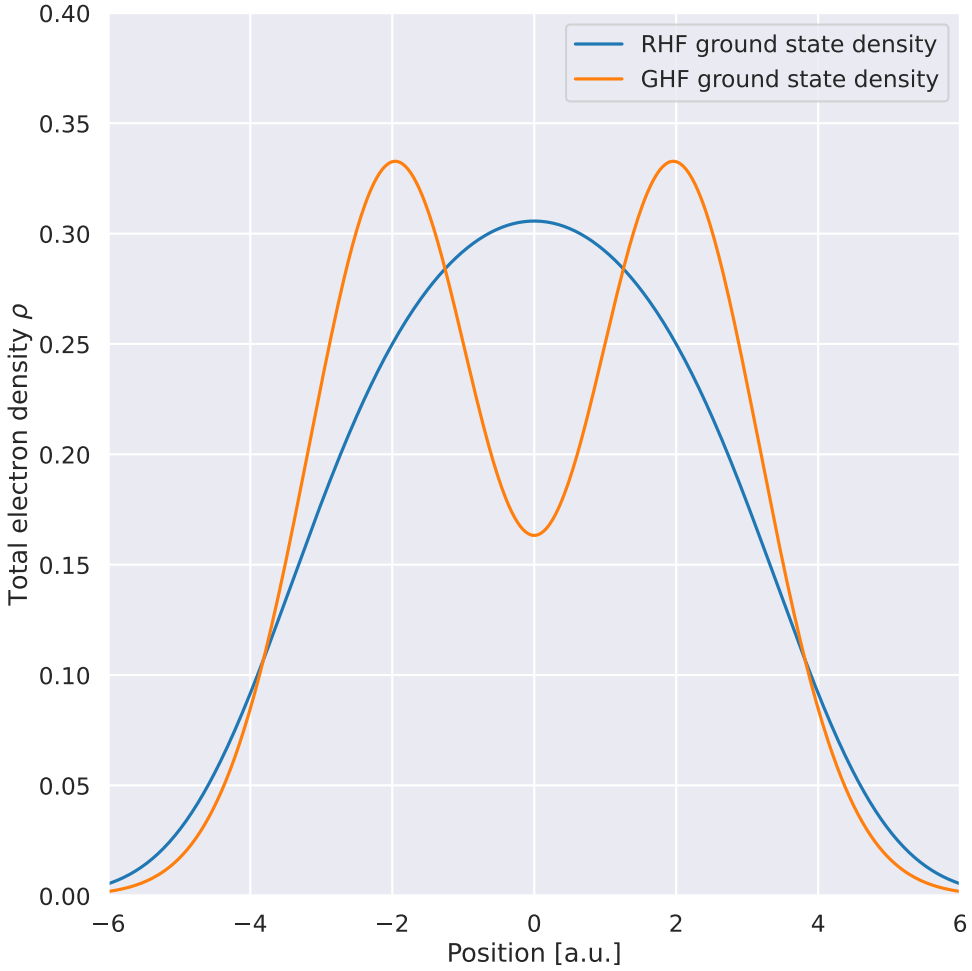

Figure 2: *Total spatial electron density for the RHF and the GHF solutions. Calculations were made on the discretised grid described in section 2.7.*

First, we observe that the RHF solution is identical to the HF-solution found by Zanghellini et al.[1], while the GHF solution resembles the shape of their FCI solution qualitatively (but it is not identical), as it has two maxima and a local minimum at $x = 0$. Both solutions are symmetric, as can be expected in a symmetric potential.

3.3 Molecular orbital solutions

A graph comparing the molecular orbital solutions for the GHF and the RHF solution is found in figure 3.

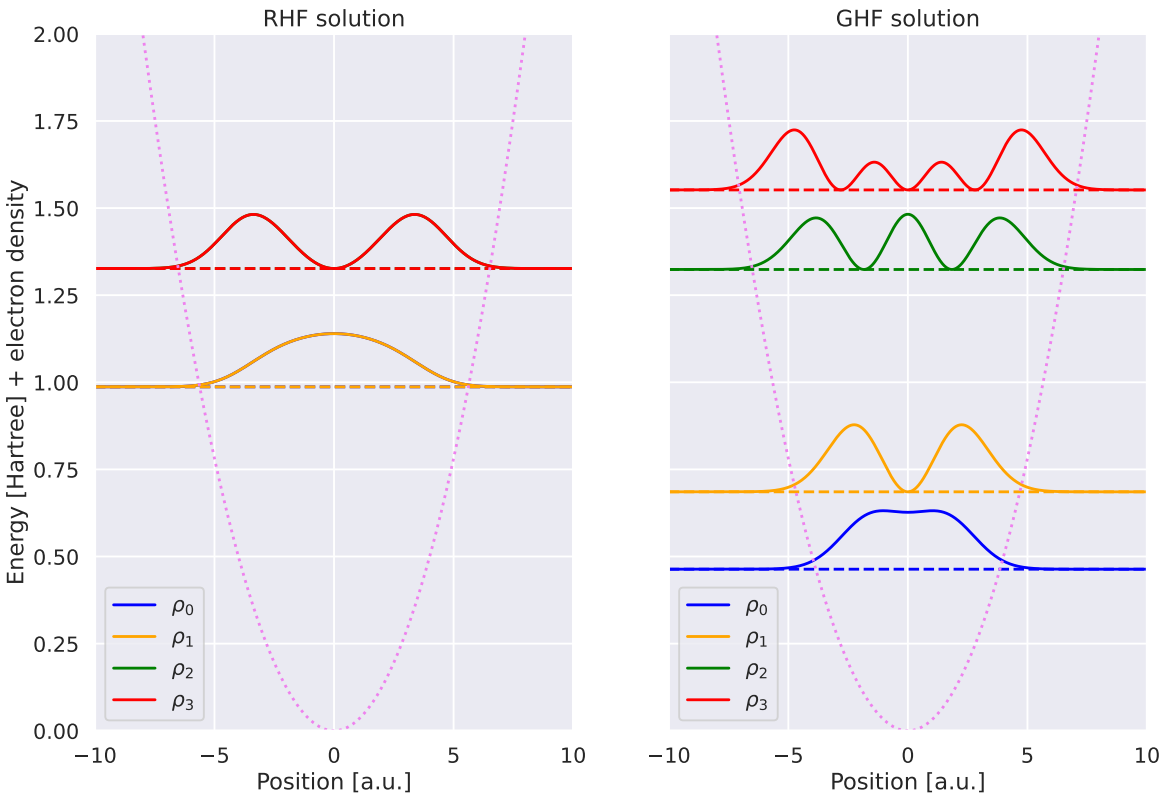

Figure 3: *Molecular orbital spatial densities plotted at their energy for the 4 molecular orbitals of lowest eigenvalue. In the left figure, the graphs ρ_0, ρ_2 are hidden behind the graphs ρ_1, ρ_3.*

As expected, the molecular orbitals with lowest eigenvalues differ quite a lot. Their eigenvalues can be perceived as a measure of their individual energy.[5] For the RHF solution, the first pair and the second pair of states have the same energy and density by construction, as discussed in section 2.5. For the GHF solution, we see that we get 4 quite different lowest-lying orbitals. With the discussion of section 2.5 in mind this is not surprising either, because the reduced energy comes at the cost of mixing spin so that the molecular orbitals do not inherit the spin degeneracy of the atomic orbitals.

3.4 Time-dependent overlap and dipole moment

We plotted the time-dependent overlap between the initial HF ground state, $|\Phi_0\rangle \equiv |\Phi[t=0]\rangle$, and the TDHF time-evolved state $|\Phi[t]\rangle$ under the influence of a time-dependent laser potential, which is first set to be constantly on (that is, $T = \infty$, which is the same system as in [1]). This is shown in figure 4. We also plotted the time-dependent dipole moment, which is shown in figure 5.

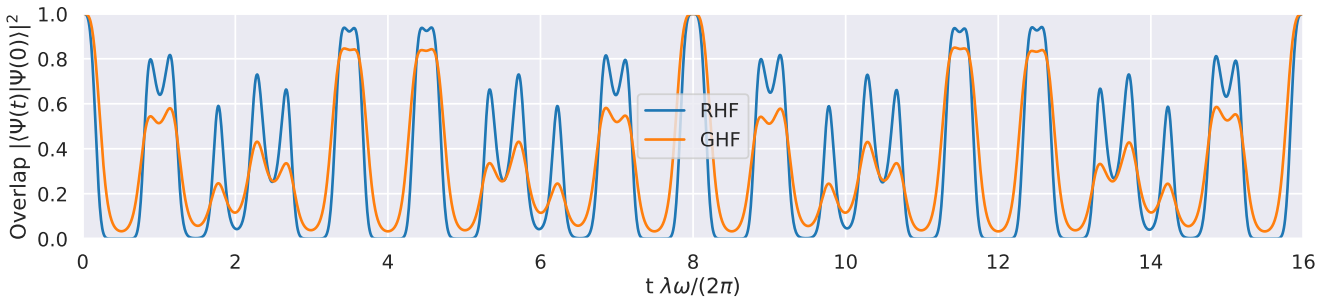

Figure 4: *Overlap* $|\langle\Psi_0|\Psi[t]\rangle|^2$ *with the laser turned on. The time axis is scaled in units of* $\frac{2\pi}{\lambda\omega}$*, which equals the period of the laser.*

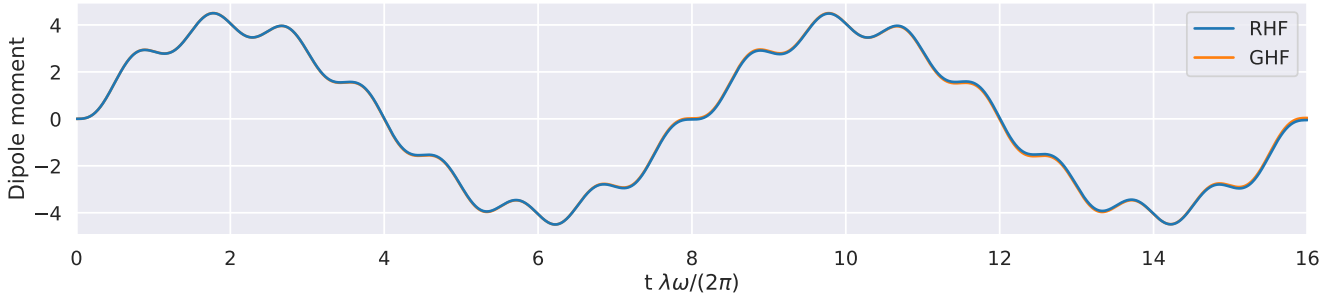

Figure 5: *Time evolution of the system dipole moment* $-\langle\Psi[t]|x|\Psi[t]\rangle$ *with the laser turned on. The time axis is scaled in the same way as figure 8.*

First of all, we observe again that the overlap in the time span $[0, 4]$ for the RHF solution is completely identical to the result by Zanghellini et al in [1]. It is also quite interesting to observe that our GHF solution has the same qualitative shape as the FCI solution found by [1], albeit there are quantitative differences, which is expected as we do not actually operate with the full FCI solution.

Furthermore, an interesting observation is that the time span $[4, 8]$ is a "mirror" of the time span $[0, 4]$ for both the GHF and the RHF state . This can be explained by an animation of the system's spatial density as a function of time, which is available online[6]. The density moves "to the left" before moving back "to the right". The states' overlap repeats at time $t = 8\frac{2\pi}{\lambda\omega}$, which means that it is a function with period $8\frac{2\pi}{\lambda\omega}$. This is what we see in the plot of the dipole moment, as the dimensionless dipole moment is nothing but the negative of the expected position $\langle\Phi|x|\Phi\rangle$. The particle oscillates to the left, then to the right. We see that the two graphs for the RHF and the GHF solution overlap almost perfectly, showing that both solutions move in essentially the same manner.

However, the two graphs in figure 5 do not overlap perfectly, as can be seen best at $t = 16\frac{2\pi}{\lambda\omega}$. Neither solution returns exactly to zero, but lie around -0.05, which indicates that our calculated dipole moment, as well as our overlap, is not perfectly periodic – this is however a consequence of errors in the numerical integration, as the model Hamiltonian (2.3) and hence our model system *is* perfectly periodic. Doubling the number of basis functions to $M = 40$, and doubling the grid size to $x \in [-20, 20]$, the error at $t = 16\frac{2\pi}{\lambda\omega}$ reduces to -0.002. Interestingly, this also removes the "jiggling" from the spatial density animation, which is also available online[7], indicating that the laser simply makes the system move from the left to the right, without inducing any additional fluctuations, in the atomic orbital basis set limit $M \to \infty$.

[6] https://github.com/schraderSimon/ComputationalPhysics2-Project2/blob/main/figures/animation.gif
[7] https://github.com/schraderSimon/ComputationalPhysics2-Project2/blob/main/figures/animation_high.gif

3.5 Time dependent dipole moment and Fourier transform

We proceeded to simulate the behaviour of our system after the laser is turned off. To do this we turned off the laser at the time $t = T = \frac{2\pi}{\lambda\omega}$ as introduced in 2.1. We know from figure 4 that the overlap $\langle\Phi_0|\Phi[t]\rangle$ at $t = T$ is neither zero nor one, so we expect the system to continue evolving with an expected energy higher than the initial ground state energy E_{HF}.

We simulated for a total time $\Delta t = 201T$, that is, for one period T of the laser and then a time span of $200T$ with the laser turned off. This number was chosen to get a spacing of $\Delta\omega_d = 0.010$ when doing Fourier analysis. The dipole moment as function of time is shown in figure 6 and its Fourier transform is shown in figure 7.

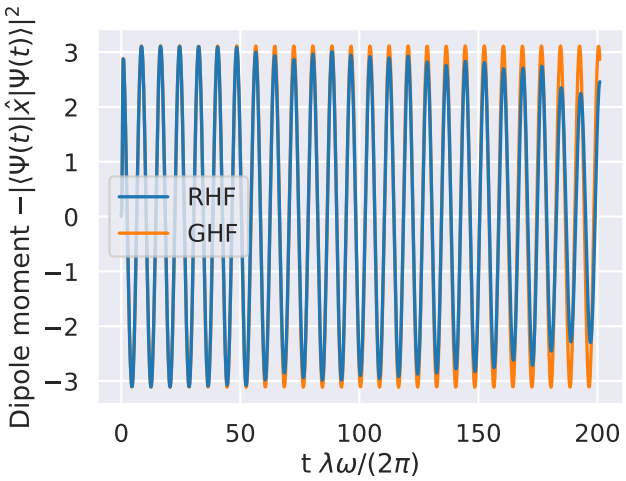

Figure 6: *Time evolution of the system dipole moment with the laser turned off at* $t = T = \frac{2\pi}{\lambda\omega}$, *which is equivalent to* 1 *on the time axis.*

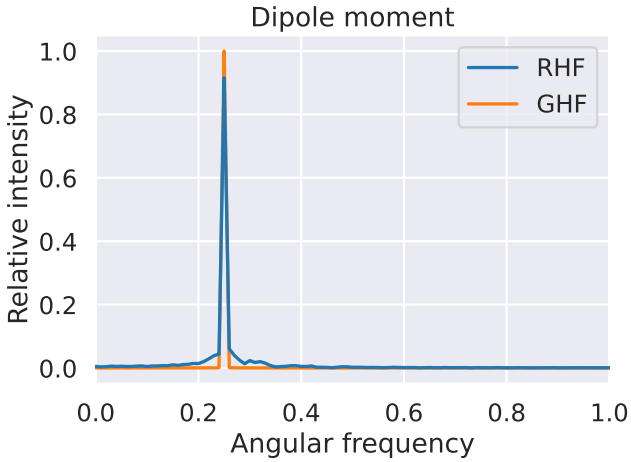

Figure 7: *Fourier transform (absolute value) of the dipole moment in figure 6. The amplitude is relative to the highest peak.*

In the Fourier transform of the dipole moment, we see that both solutions have a single peak at an angular frequency $\omega_d = 0.25 \pm 0.01$. The dipole moment plots in figure 6 shows that both the RHF and the GHF solution are dominated by one frequency, but the RHF plot is slightly less regular, indicating that at least one other frequency is mixed in. The Fourier transforms in figure 7 confirm this, as the peak for the RHF solution is somewhat more spread. These results anyway match with the Harmonic Potential Theorem discussed at the end of section 2.6, which predicts a sole peak

at $\omega_d = \omega$ – the system thus behaves like a harmonic oscillator with an elevated ground state, for which we only observe transitions $\langle n|\, x\, |m\rangle = C(\delta_{n,m+1} + \delta_{n,m-1})$ for some constant C. From a computational perspective, we expect the error in the RHF solution of figures 6 and 7 to stem from numerical inaccuracy due to a too small atomic orbital basis set. To verify this, we again increase the resolution by doubling the the number of atomic orbitals M and the grid length. In that case, the time dependent dipole moment plots are virtually identical for both RHF and GHF, and there is only one single, clear peak at $\omega_d = 0.25$ for both the RHF and GHF solutions. This can be seen in figures 9 and 10 in appendix B.

Figure 8 shows the Fourier transform of the overlap $|\langle\Psi[T]|\Psi[T+t]\rangle|^2$ as defined in eq. (2.52) when the laser is turned off at $t = T = \frac{2\pi}{\lambda\omega}$.

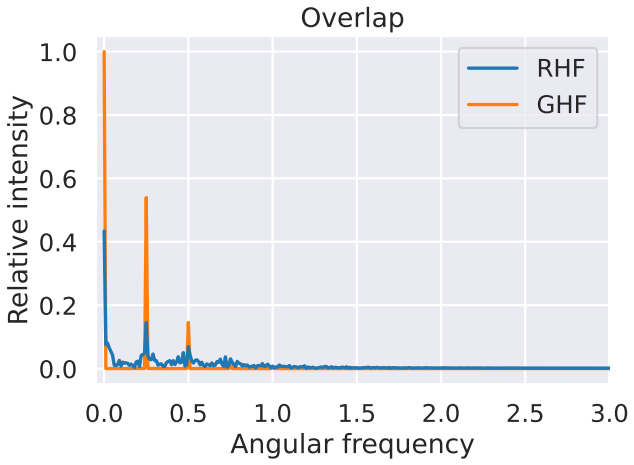

Figure 8: *Fourier transform (absolute value) of the overlap with the laser turned off at* $t = T = \frac{2\pi}{\lambda\omega}$. *The amplitude is relative to the highest peak.*

The Fourier transform of the overlap seems to have peaks at $\omega_\Gamma = n\omega \pm 0.01$ for $n \in \{1, 2, 3, 4, 5\}$ (the peaks for $n \in \{3, 4, 5\}$ are barely visible in the plot) for the GHF solution, and $n \in \{0, 1, 2\}$ for the RHF solution (which has some inaccuracies that did not disappear when increasing the basis set size). This again matches with the Harmonic Potential Theorem. From this, we see that also higher-lying states than the first excited state are populated, but because the peak amplitude gets smaller for increasing values of ω_Γ, we observe that their occupancy is smaller.

It is surprising to see that the Hartree-Fock approximation, both time-independent and time-dependent, manages to reproduce expected behaviour of real systems predicted by the Harmonic Potential Theorem despite being a rather limited approximation. Especially given the fact that time evolution as derived from time-dependent Hartree-Fock theory in section 2.4 does not follow the Schrödinger equation exactly, it is quite interesting to see that the approximation still seems sufficient to obtain information about real systems, as in the case of the system (2.3) of this report.

4 Conclusion

We have derived and implemented an object-oriented GHF (as well as RHF) solver for N electrons in a harmonic trap and a time-dependent GHF solver for the time evolution of the system when subjected to a laser in the dipole approximation. Using the same parametric values as in [1], we found the ground state energy for the RHF solution to be 1.1796 a.u., matching their results. We also found a much lower ground state energy with our GHF solver with the value 0.84504 a.u. Our corresponding GHF ground state density turns out to resemble their FCI solution qualitatively, with a local minimum in the middle of the trap and two local, symmetric maxima. This shows that the

simple Hartree-Fock solution actually can describe the physical ground state better than what [1] indicates – at the price that the system might be spin contaminated. We were surprised by the difference in the ground state energy between the RHF and the GHF solutions, which indicates that a much better approximation to the spatial part of the ground state can be made within the one-determinant picture when spin symmetry is neglected.

Again using the same parametric values for the laser as used in [1], we found the same time evolution (in terms of time-dependent overlap with the non-evolved state at $t = 0$) under the influence of the laser of the RHF state as they did with their HF solution. Furthermore, the time evolution of our GHF solution resembles their FCI time evolution qualitatively, especially observing that the overlap with the non-time developed state at $t = 0$ never becomes zero for the GHF solution, as does their FCI solution. Analysing the partial frequencies of both the RHF and GHF solutions after turning off the laser, we found that the Fourier transform of the time-dependent dipole moment has a single peak at the value of the harmonic oscillator frequency $\omega = 0.25 \pm 0.01$ a.u., while the Fourier transform of the time-dependent overlap has peaks at integer multiples of ω. This shows that transition between energy states can only occur in definite quanta of $\omega = 0.25$ a.u., confirming that the Harmonic Potential Theorem holds also for our approximate Hartree-Fock states.

Finally, we observed that increasing the size of the atomic orbital basis set leads to improved results, as the peaks in the Fourier transforms get much sharper when it is increased, and the dipole moment of both the RHF and the GHF solutions become increasingly periodic.

In this article, we only considered 2 electrons. Different, interesting results could clearly be obtained using a higher number of electrons N. The code developed here is general with respect to N, so that such results are easily available. It would also be interesting to expand the code and consider systems in 2 and 3 dimensions. We have only used the Hartree-Fock theory, so more exact methods such as the Coupled-Cluster or Configuration Interaction methods could give more physically correct results. We did not explicitly measure the degree of spin contamination in the GHF solution, which would be interesting to examine. Finally, considering strong lasers and approximations more accurate than the dipole approximation could lead to other interesting observations.

APPENDIX

A Derivations

A.1 Time-independent Hartree-Fock equations

We want to find the lowest energy bound from a trial Slater determinant by minimising the Lagrangian L given in (2.19) with respect to the coefficients of the molecular orbitals defined through (2.16). We first introduce a small variation δC_{ek} to a specific coefficient C_{ek} (for the specific indices e and k). The resulting variation in the Lagrangian should be zero for it to be at a minimum with respect to this coefficient. The variation in the Lagrangian is given by

$$\begin{aligned}\delta L &= 2\,\mathrm{Re}\left[\sum_a^M C_{ak}^* \delta C_{ek} \langle\chi_a|\, h\,|\chi_e\rangle + \sum_{a,b,c}^M \sum_i^N C_{ak}^* C_{bi}^* \delta C_{ek} C_{ci} \langle\chi_a\chi_b||\chi_e\chi_c\rangle - \sum_i^N \alpha_{ik}^* C_{ei}^* \delta C_{ek}\right] \\ &= 2\,\mathrm{Re}\left[\left(\sum_a^M C_{ak}^* \langle\chi_a|\, h\,|\chi_e\rangle + \sum_{a,b,c}^M \sum_i^N C_{ak}^* C_{bi}^* C_{ci} \langle\chi_a\chi_b||\chi_e\chi_c\rangle - \sum_i^N \alpha_{ik}^* C_{ei}^*\right) \delta C_{ek}\right],\end{aligned}$$

and because the variation δC_{ek} is arbitrary, the expression in the inner parantheses should strictly be zero. The complex conjugate of this results in the equation

$$\sum_a^M \langle\chi_e|\, h\,|\chi_a\rangle\, C_{ak} + \sum_{a,b,c}^M \sum_i^N C_{bi} C_{ci}^* \langle\chi_e\chi_c||\chi_a\chi_b\rangle C_{ak} = \sum_i^N C_{ei}\alpha_{ik},$$

which can be simplified by introducing the *Fock matrix* by its elements

$$F_{ab} = \langle\chi_a|\, h\,|\chi_b\rangle + \sum_{c,d}^M \sum_i^N C_{ci} C_{di}^* \langle\chi_a\chi_d||\chi_b\chi_c\rangle, \tag{A1}$$

to get

$$\sum_a^M F_{ea} C_{ak} = \sum_i^N C_{ei}\alpha_{ik}.$$

This equation should hold not only for two specific indices e and k, but for *all* indices e and k, as variation of any of the coefficients should result in zero variation of the Lagrangian at the minimum. In other words the above equation is actually a set of equations which can then be recast as a matrix equation

$$\boxed{F}\boxed{C} = \boxed{C}\boxed{\alpha}, \tag{A2}$$

where $\boxed{F}$ is the $M \times M$ Fock matrix as defined in (A1), $\boxed{C}$ is the $M \times N$ coefficient matrix of the molecular orbital coefficients introduced in (2.16) and $\boxed{\alpha}$ is the $N \times N$ matrix of Lagrange multipliers related to the orthonormal constraint on the molecular orbitals.

The matrix equation above can be recast to a simpler form by exploiting the hermiticity of $\boxed{\alpha}$. To see that this matrix is Hermitian, we proceed to minimise the Lagrangian (2.19) with respect to the Lagrange multipliers, which simply yields the orthonormal constraint itself, $\boxed{C}^\dagger\boxed{C} = \boxed{I}$. Multiplying now the equation (A2) from the left by $\boxed{C}^\dagger$, and using this orthonormality we end up with

$$\boxed{\alpha} = \boxed{C}^\dagger\boxed{F}\boxed{C} \tag{A3}$$

which shows that $\boxed{\alpha}$ is indeed Hermitian. Now, note that the Fock matrix $\boxed{F}$ as introduced in (A1) will *not be affected* by a unitary transformation of $\boxed{C}$ such that $\boxed{C'} = \boxed{C}\boxed{U}$ for any unitary $N \times N$ matrix $\boxed{U}$. To see this we introduce the so-called *density matrix* defined as

$$\boxed{P} = \boxed{C}\boxed{C}^\dagger. \tag{A4}$$

The Fock matrix elements are then really only dependent on this density matrix,

$$F_{ab} = \langle \chi_a | \, h \, | \chi_b \rangle + \sum_{c,d}^{M} P_{cd} \langle \chi_a \chi_d || \chi_b \chi_c \rangle. \tag{A5}$$

But from the definition (A4) it is clear that the density matrix, and hence also the Fock matrix, is unaffected by the unitary transformation, as

$$\boxed{P'} = \boxed{C'}\boxed{C'}^\dagger = \boxed{C}\boxed{U}\boxed{U}^\dagger\boxed{C}^\dagger = \boxed{C}\boxed{C}^\dagger = \boxed{P}.$$

The Lagrange multiplier matrix $\boxed{\alpha}$ however *will* be affected by the transformation – in fact we will choose the very specific transformation $\boxed{U}$ that diagonalises it,

$$\boxed{U}^\dagger \boxed{\alpha} \boxed{U} = \boxed{\varepsilon}, \tag{A6}$$

where $\boxed{\varepsilon}$ is a diagonal matrix with the real eigenvalues of $\boxed{\alpha}$ along its diagonal. This constraint on $\boxed{U}$ can always be fulfilled for a Hermitian matrix such as $\boxed{\alpha}$. Multiplying (A2) from the right by $\boxed{U}$ and omitting the primes, we finally obtain

$$\boxed{F}\boxed{C} = \boxed{C}\boxed{\varepsilon}, \tag{A7}$$

which is much simpler as $\boxed{\varepsilon}$ is a diagonal matrix. This equation lies at the core of Hartree-Fock theory and is known as the Rothaan-Hall equation. It is the matrix formulation of the more abstract Hartree-Fock equations.

A comment is in order on the unitary transformation and omission of primes above. As shown, both the density matrix $\boxed{P}$ and the Fock matrix $\boxed{F}$ is unaffected by a unitary transformation of the coefficients $\boxed{C}$. This is an expression of the more general fact that unitary transformations of the molecular orbitals will not affect any of the real physics of the system. The expression for the expected value of any observable of the system turns out only to depend on $\boxed{C}$ through $\boxed{P}$, as becomes apparent in section 2.6. We are hence free to consider a coefficient matrix $\boxed{C}$ from the start which already makes the matrix equation (A2) take the diagonal form of the Roothaan-Hall equation (A7) without further transformations.

A.2 Time-dependent Hartree-Fock equations

We now want to minimise the action integral (2.27) of the time-dependent Lagrangian L given in (2.26) with respect to both the coefficients of the molecular orbitals defined through (2.16) and the Lagrange multipliers α^*_{ij}. In a similar fashion to section A.1 we first introduce a small variation δC_{ek} to a specific coefficient C_{ek}, which is this time a function of time that is zero at the boundaries (at the initial and final point of the time span). The resulting variation in the the action is

$$\begin{aligned}
\delta S &= \int \left(2 \,\mathrm{Re} \left[\left(\sum_a^M C^*_{ak} F_{ea} - \sum_i^N C^*_{ei} \alpha^*_{ik} \right) \delta C_{ek} \right] - \iota \left(\delta C^*_{ek} \dot{C}_{ek} + C^*_{ek} \delta \dot{C}_{ek} \right) \right) \delta t \\
&= \int \left(2 \,\mathrm{Re} \left[\left(\sum_a^M C^*_{ak} F_{ea} - \sum_i^N C^*_{ei} \alpha^*_{ik} \right) \delta C_{ek} \right] - \iota \left(\delta C^*_{ek} \dot{C}_{ek} - \dot{C}^*_{ek} \delta C_{ek} \right) \right) \delta t \\
&= \int \left(2 \,\mathrm{Re} \left[\left(\sum_a^M C^*_{ak} F_{ea} - \sum_i^N C^*_{ei} \alpha^*_{ik} \right) \delta C_{ek} \right] + \iota \dot{C}^*_{ek} \delta C_{ek} - \iota \dot{C}_{ek} \delta C^*_{ek} \right) \delta t \\
&= 2 \int \mathrm{Re} \left[\left(\iota \dot{C}^*_{ek} + \sum_a^M C^*_{ak} F_{ea} - \sum_i^N C^*_{ei} \alpha^*_{ik} \right) \delta C_{ek} \right] \delta t,
\end{aligned}$$

where we define the now time-dependent Fock matrix elements F_{ab} through the now time-dependent density matrix $\boxed{P}$ as given in (2.21) and (2.22). Since the variation δC_{ek} is arbitrary we can once again deduce that the complex conjugate of the expression in the inner parantheses should be zero to get the matrix equation

$$\iota\dot{\boxed{C}} = \boxed{F}\boxed{C} - \boxed{C}\boxed{\alpha}. \tag{A8}$$

Proceeding to minimise the action integral with respect to the Lagrange multipliers, we simply get the orthonormal constraint $\boxed{C}^\dagger\boxed{C} = \boxed{I}$ which should be fulfilled at all times. From this it is possible to find an expression for $\boxed{\alpha}$ by multiplying (A8) from the left by $\boxed{C}^\dagger$, which results in

$$\boxed{\alpha} = \boxed{C}^\dagger\boxed{F}\boxed{C} - \iota\boxed{C}^\dagger\dot{\boxed{C}}. \tag{A9}$$

Inserting this back into (A8) we end up with

$$\iota\Big(\boxed{I} - \boxed{P}\Big)\dot{\boxed{C}} = \Big(\boxed{I} - \boxed{P}\Big)\boxed{F}\boxed{C},$$

which looks difficult to decouple as the matrix $\Big(\boxed{I} - \boxed{P}\Big)$ is a projection matrix and hence singular. However, a unitary transformation of the coefficients $\boxed{C}$ once again comes to our rescue. As in derivation A.1, such a unitary transformation does not affect the density matrix $\boxed{P}$ nor the Fock matrix $\boxed{F}$. This time however the transformation is time-dependent, so we can actually put *two* constraints on it,

$$\iota\boxed{C'}^\dagger\dot{\boxed{C'}} = \boxed{C'}^\dagger\boxed{F}\boxed{C'} = \boxed{0}, \tag{A10}$$

as shown in [7]. With these transformed coefficients, the projected equation above reduces significantly, as the left hand side becomes

$$\iota\Big(\boxed{I} - \boxed{P}\Big)\dot{\boxed{C'}} = \iota\dot{\boxed{C'}} - \boxed{P}\dot{\boxed{C'}} = \iota\dot{\boxed{C'}} - \iota\boxed{C'}\boxed{C'}^\dagger\dot{\boxed{C'}} = \iota\dot{\boxed{C'}}$$

while the right hand side becomes

$$\Big(\boxed{I} - \boxed{P}\Big)\boxed{F}\boxed{C'} = \boxed{F}\boxed{C'} - \boxed{P}\boxed{F}\boxed{C'} = \boxed{F}\boxed{C'} - \boxed{C'}\boxed{C'}^\dagger\boxed{F}\boxed{C'} = \boxed{F}\boxed{C'}.$$

In total then, we choose this transformation of $\boxed{C}$, omit the primes and end up with

$$\iota\dot{\boxed{C}} = \boxed{F}\boxed{C}. \tag{A11}$$

We will refer to this equation as the time-dependent Roothaan-Hall equation.

A.3 Spin-restricted Hartree-Fock equations

We examine how the derivations of sections A.1 and A.2 change when the molecular orbitals $|\phi_i\rangle$ are spin-restricted as in (2.34). In this section we use the letters s and p for summation indices running through $\downarrow$ and $\uparrow$, generalising the notation introduced in section 2.5. Firstly, note that the expression (2.17) for the energy bound $\langle\Phi|H|\Phi\rangle$ should be written

$$\begin{aligned}\langle\Phi|H|\Phi\rangle &= \sum_{i}^{\frac{N}{2}}\sum_{s}\langle\phi_i^s|h|\phi_i^s\rangle + \frac{1}{2}\sum_{i,j}^{\frac{N}{2}}\sum_{s,p}\big\langle\phi_i^s\phi_j^p\big|\big|\phi_i^s\phi_j^p\big\rangle \\ &= \sum_{a,b}^{\frac{M}{2}}\sum_{i}^{\frac{N}{2}}\sum_{s}C_{ai}^*C_{bi}\,\langle\chi_a^s|\,h\,|\chi_b^s\rangle + \frac{1}{2}\sum_{a,b,c,d}^{\frac{M}{2}}\sum_{i,j}^{\frac{N}{2}}\sum_{s,p}C_{ai}^*C_{bj}^*C_{ci}C_{dj}\langle\chi_a^s\chi_b^p||\chi_c^s\chi_d^p\rangle,\end{aligned} \tag{A12}$$

as we no longer want to merge the sums over spatial and spin parts. Rather, we want to write them out explicitly like this in order to *sum out* the spin parts and obtain any resulting factors. To this end we note that

$$\begin{aligned}\sum_s \langle \chi_a^s | \, h \, | \chi_b^s \rangle &= \sum_s \langle s|s \rangle \, \langle \psi_a | \, h \, | \psi_b \rangle \\ &= 2 \, \langle \psi_a | \, h \, | \psi_b \rangle \, ,\end{aligned} \tag{A13}$$

so the first term in (A12) gets an extra factor of 2. However, looking at the second term we can no longer keep the notation (2.13) introduced back in section 2.2, because the negative part disappears in the case of opposite spins, while the positive part remains:

$$\begin{aligned}\sum_{s,p} \langle \chi_a^s \chi_b^p || \chi_c^s \chi_d^p \rangle &= \sum_{s,p} \Big(\langle \chi_a^s \chi_b^p | \, u \, | \chi_c^s \chi_d^p \rangle - \langle \chi_a^s \chi_b^p | \, u \, | \chi_d^p \chi_c^s \rangle \Big) \\ &= \sum_{s,p} \Big(\langle s|s \rangle \, \langle p|p \rangle \, \langle \psi_a \psi_b | \, u \, | \psi_c \psi_d \rangle - \langle s|p \rangle \, \langle p|s \rangle \, \langle \psi_a \psi_b | \, u \, | \psi_d \psi_c \rangle \Big) \\ &= 4 \, \langle \psi_a \psi_b | \, u \, | \psi_c \psi_d \rangle - 2 \, \langle \psi_a \psi_b | \, u \, | \psi_d \psi_c \rangle \, .\end{aligned} \tag{A14}$$

Thus in total, the energy bound (A12) becomes

$$\langle \Phi | H | \Phi \rangle = \sum_{a,b}^{\frac{M}{2}} \sum_{i}^{\frac{N}{2}} 2 C_{ai}^* C_{bi} \, \langle \psi_b | \, h \, | \psi_a \rangle + \sum_{a,b,c,d}^{\frac{M}{2}} \sum_{i,j}^{\frac{N}{2}} C_{ai}^* C_{bj}^* C_{ci} C_{dj} \Big(2 \, \langle \psi_b \psi_d | \, u \, | \psi_a \psi_c \rangle - \langle \psi_b \psi_d | \, u \, | \psi_c \psi_a \rangle \Big) \tag{A15}$$

and we can proceed to minimise it with respect to the Variational Principle (2.15) or time similarly to sections A.1 and A.2. However, note that the *only difference* between (A15) and (2.17) is that the right side is doubled, the dimensions M and N are halved and the atomic orbitals $|\chi_a\rangle$ are replaced with their spatial part $|\psi_a\rangle$. It follows that the minimisations in sections A.1 and 2.4 are still valid. $\boxed{C}$ will be an $\frac{M}{2} \times \frac{N}{2}$ matrix of (degenerate) coefficients which now describe *two* molecular orbitals of opposite spin through (2.34), $\boxed{P}$ is an $\frac{M}{2} \times \frac{M}{2}$ matrix still defined through (2.22) while the Fock matrix $\boxed{F}$ is an $\frac{M}{2} \times \frac{M}{2}$ matrix with elements

$$F_{ab} = \langle \psi_a | \, h \, | \psi_b \rangle + \sum_{c,d}^{\frac{M}{2}} P_{cd} \Big(2 \, \langle \psi_a \psi_d | \, u \, | \psi_b \psi_c \rangle - \langle \psi_a \psi_d | \, u \, | \psi_c \psi_b \rangle \Big) . \tag{A16}$$

With these new definitions in mind however, the Roothaan-Hall equation (2.20) as well as the time-dependent Roothaan-Hall equation (2.28) take the exact same form as in the general spin-unrestricted case. To calculate expected values such as the energy (2.23) or any other expected value given in section 2.6 one should keep in mind that the dimensions and matrix elements change as described above, but other than that, they will take the same form as well.

B Figures

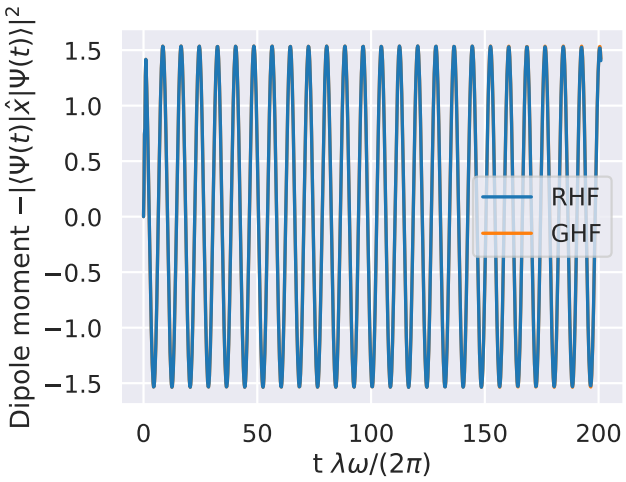

Figure 9: *Time evolution of the system dipole moment with the laser turned off at* $t = T = \frac{\lambda\omega}{2\pi}$. *Here* $M = 40$, *and the grid length is also doubled with respect to figure 6. The GHF solution is hidden behind the RHF solution.*

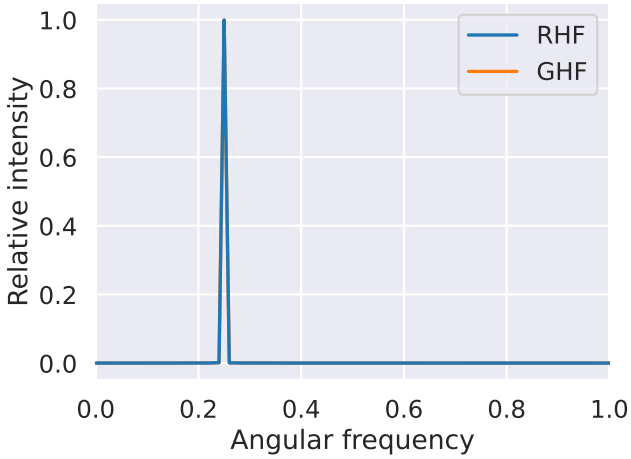

Figure 10: *Fourier transform (absolute value) of the dipole moment in figure 9. The intensity is relative to the highest peak. Here,* $M = 40$, *and the grid length is doubled. The GHF solution is hidden behind the RHF solution.*

References

[1] Zanghellini, J. et al. "Testing the multi-configuration time-dependent Hartree–Fock method". In: *Journal of Physics B: Atomic, Molecular and Optical Physics* 37 (Jan. 2004), p. 763. DOI: 10.1088/0953-4075/37/4/004 (cit. on pp. 1, 2, 14, 16–19, 21, 22).

[2] Brey, L., Johnson, N. F., and Halperin, B. I. "Optical and magneto-optical absorption in parabolic quantum wells". In: *Physical Review B* 40.15 (1989), pp. 10647–10649. DOI: 10.1103/physrevb.40.10647 (cit. on pp. 1, 14).

[3] Harris, C. R. et al. "Array programming with NumPy". In: *Nature* 585 (2020), pp. 357–362. DOI: 10.1038/s41586-020-2649-2 (cit. on pp. 1, 15).

[4] Virtanen, P. et al. "SciPy 1.0: Fundamental Algorithms for Scientific Computing in Python". In: *Nature Methods* 17 (2020), pp. 261–272. DOI: 10.1038/s41592-019-0686-2 (cit. on pp. 1, 15).

[5] Szabo, A. and Ostlund, N. S. *Modern Quantum Chemistry: Introduction to Advanced Electronic Structure Theory*. First. Dover Publications, Inc., 1982 (cit. on pp. 10, 18).

[6] Plasser, F. et al. "Efficient and Flexible Computation of Many-Electron Wave Function Overlaps". In: *Journal of Chemical Theory and Computation* 12.3 (2016), pp. 1207–1219. DOI: 10.1021/acs.jctc.5b01148 (cit. on p. 12).

[7] Alon, O. E., Streltsov, A. I., and Cederbaum, L. S. "Multiconfigurational time-dependent Hartree method for bosons: Many-body dynamics of bosonic systems". In: *Phys. Rev. A* 77 (3 Mar. 2008), p. 033613. DOI: 10.1103/PhysRevA.77.033613. URL: https://link.aps.org/doi/10.1103/PhysRevA.77.033613 (cit. on p. 25).